

Individual and Collective Behaviors in Soft Robot Worms Inspired by Living Worm Blobs

Carina Kaeser¹, Junghan Kwon^{2,3}, Elio Challita², Harry Tuazon⁴,
Robert J. Wood², Saad Bhamla⁴, Justin Werfel²

Abstract—California blackworms constitute a recently identified animal system exhibiting unusual collective behaviors, in which dozens to thousands of worms entangle to form a “blob” capable of actions like locomotion as an aggregate. In this paper we describe a system of pneumatic soft robots inspired by the blackworms, intended for the study of collective behaviors enabled and mediated by such physical entanglement. Both the robots and worms have high aspect ratio ($\approx 1:50$), intertwine in complex 3D configurations, operate both in air and underwater, and can locomote both individually and as a collective. We demonstrate and characterize locomotion for both individual robots and entangled blobs, explore the tunability of entanglement strength, and compare these to the analogous versions in living worms. The robots provide a testbed for studying mechanisms underlying behaviors observed in worm blobs, as well as serving as a platform for studies of novel collective behaviors based on physical entanglement.

I. INTRODUCTION

Swarm robotics is often inspired by the collective behavior of social animals like birds, fish, and bees. The corresponding robot systems share many features with the animals, such as collective abilities beyond those of the individuals, robustness to loss of agents, and scalability to large numbers [1]–[3]. Most work in swarm robotics focuses on traditional rigid-bodied robots, and topics like exploration and flocking, with physically separate robots spread out across a space [3].

A recently identified collective animal system, just starting to be explored by biologists as well as roboticists, is that of California blackworms (*Lumbriculus variegatus*), centimeter-scale worms that form entangled “blobs” of dozens to many thousands of individuals [4] (Fig. 1A, B). Sophisticated collective behaviors exhibited by these worms, such as directed locomotion of a blob, may rely on both the flexibility of the worms and their physical entanglement [5]–[7]. Artificial systems inspired by the worms, able to operate both as individuals and as physically linked collectives, could similarly demonstrate advantages like parallel operation in the former mode (e.g., exploration of a large space) and capabilities beyond those of individuals in the latter (e.g., crossing a gap). Still more complex abilities, such as a blob

climbing or “chimneying” through coordinated actuation, may be possible for systems with such properties even if not observed in nature.

In this work we present a soft robotic analogue to the worm blob system, in which pneumatically actuated, independently controlled soft robots with worm-like aspect ratio ($\approx 1:50$) can operate both as individual agents and as entangled collectives (Fig. 1C–E). We demonstrate and quantitatively characterize locomotion in both the individual and collective states, and characterize the cohesive strength of both robot and worm blobs as the rigidity of the individual agents is varied. The robot system provides a testbed for studies of novel collective behaviors with coordination mediated through physical entanglement, as well as for evaluating hypotheses about mechanisms underlying phenomena observed in the biological system.

II. RELATED WORK

The physical interconnection fundamental to the topic of worm blobs makes the research area of self-reconfigurable modular robots [8]–[11] particularly relevant to the goals in this study. Such systems consist of modules which are independently controlled, physically connected, and capable of rearranging their connectivity. Typically the goals are for the composite robot to exhibit capabilities beyond those of the individual modules. In some cases, individual modules are not self-mobile, but achieve collective mobility through the physical interactions among units [12]–[14]. In others, each separate module is self-mobile on its own as well as when part of a composite [15]–[18], as is the case for the living worms and the goal for the robot worms. In some systems, physical connectivity provides the ability for a composite robot to traverse terrains which are unachievable for an individual (e.g., crossing a gap) [17], [18], another long-term goal of the robot system described here.

An important difference between the above systems and those considered in this paper is that the former are rigid robots. Typically they rely on that rigidity to achieve their reconfiguration and locomotion; in a few cases, rigid modules use flexible connectors to form collectives with some compliance [18], [19]. Few studies have considered collective behaviors with physically interconnected units which are soft robots. One such system, Eciton robotica, involves self-mobile individuals that are vermiform (aspect ratio $\sim 1:4$) and attach together via a connection made between the head or tail of one and the side of another [20]. Another, FoamBot, uses circular individuals that are not self-mobile and attach

¹Department of Mechanical and Process Engineering, ETH Zurich, Switzerland cakaeser@student.ethz.ch

²John A. Paulson School of Engineering and Applied Sciences, Harvard University, Boston, MA 02134, USA {jhwon, echallita, rjwood, jkwerfel}@seas.harvard.edu

³Current address: School of Mechanical Engineering, Pusan National University, Busan, Republic of Korea jhwon85@pusan.ac.kr

⁴School of Chemical and Biomolecular Engineering, Georgia Institute of Technology, Atlanta, GA 30332 {htuazon3, saadb}@gatech.edu

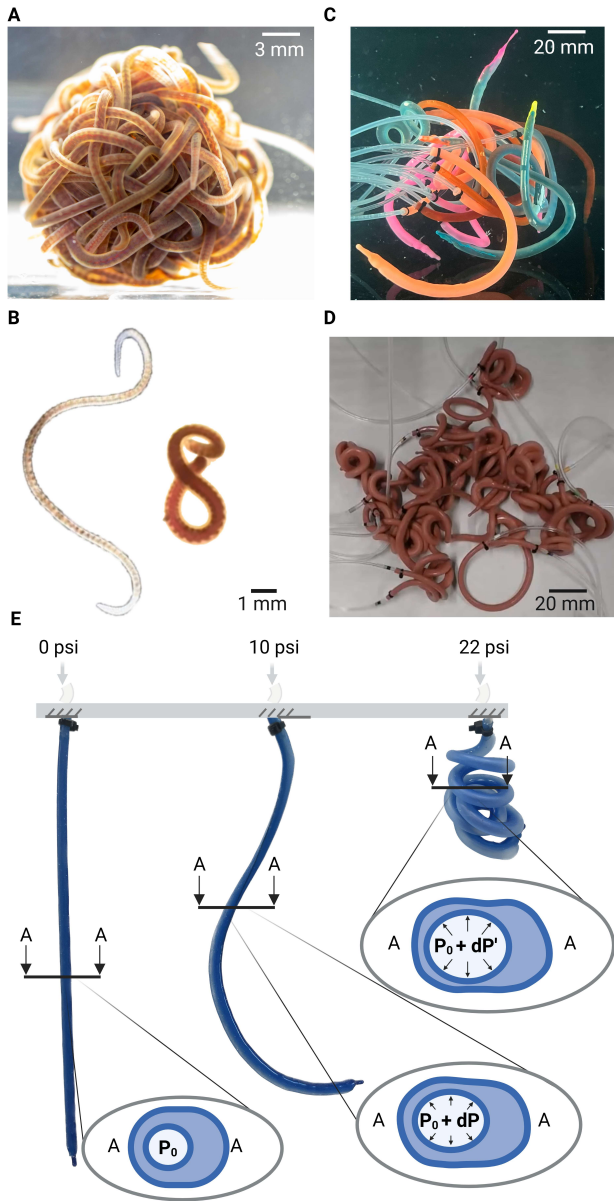


Fig. 1: (A) Living blackworm blob (~ 200 agents) underwater. (B) Two individual California blackworms, coiled to different extents. (C) Soft robotic worm blob (16 agents), made with Dragon Skin 30, underwater. Colors are to aid visual discrimination of different individuals. Thin blue tubes are pneumatic lines. (D) Soft robotic worm blob (16 agents), made with Elastosil M4601, in air. (E) Individual soft robot worm made of silicone elastomer with an embedded fluidic chamber. A–A is a cross-section of the robot, showing the asymmetric chamber geometry that produces coiling when pressurized.

to neighbors around their circumference [14], [21]. Both these systems operate in two dimensions, with limited point connections between units, whereas the blackworms and the robots emulating them move in three dimensions and can wrap around each other in topologically complex ways [22].

A recently developed gripper based on stochastic entan-

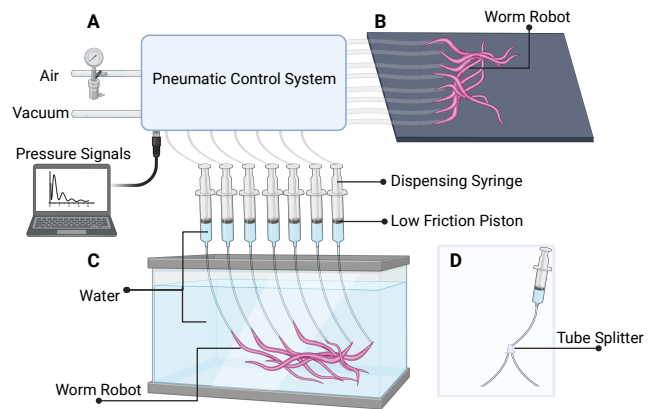


Fig. 2: Experimental setup. (A) A pressure control system drives robot operation either (B) in air (directly) or (C) underwater (via dispensing syringes to go from pneumatic to hydraulic pressure). Each channel drives either a single independent robot (for $n \leq 8$ robots) or (D) two simultaneous robots using a splitter (for $n = 16$).

glement of long filaments [23] provides a mechanical system where soft, high-aspect-ratio tendrils with asymmetric cross-section curl and intertwine in complex ways when pressurized. In that system, simultaneous pneumatic actuation of many filaments causes them to tangle around objects to be grasped as well as around each other. We adapt the design and fabrication of that system to the robotic worm blob system discussed here, in particular spatially separating the filaments from their base manifold using extended silicone tubing, and providing each with independent control, to allow each to play the role of a distinct worm.

A recent study of California blackworms identifies and characterizes certain collective behaviors in worm blobs, and provides robophysical experiments to validate hypotheses about collective locomotion, using rigid three-link robots which connect at their surfaces though they do not physically entangle [4].

III. METHODS

A. Robot Fabrication and Hardware

Each worm robot is designed as a long, slender, and flexible body shape with length ~ 280 mm and outer diameter ~ 5 mm, made of silicone elastomer, with an embedded air chamber along its length. The robot is fabricated using an open mold with a tilted curing angle [23], [24], resulting in a biased air chamber arrangement with opposite wall thicknesses of ~ 0.5 mm and ~ 2.5 mm when unpressurized. As a result, the robot curls when the internal air chamber is pressurized (Fig. 1D).

We created two sets of such robots in this study. The first, building directly on previous work [24], was made from Elastosil M4601, molded with a 1.5mm rod angled at 10° . The second was made from Dragon Skin 30, molded with a 2mm rod angled at 5° . Silicone colors (Silc Pig from Smooth-On) were added to the latter to aid in visual differentiation between the robots. The Dragon Skin robots

exhibited more variability across robots in amount of curling for a given pressure.

A custom pneumatic control system with eight independent output channels was used to actuate multiple worm robots (Fig. 2). The air pressure of each channel was regulated by pneumatic solenoid valves and an embedded PID controller. Like the living blackworms, these robots are capable of operation in air or underwater; for the latter case, a modification to the control system using additional dispensing syringes (Fig. 2C) allows hydraulic actuation of the robots without unwanted buoyancy effects that could occur for pneumatic actuation with air. We actuated robots either with a simple sine function for pressure, $P(t) = A \sin(\omega t - \phi) + B$, or a tilted sinusoid to generate different inflation and deflation speeds, $P(t) = \frac{A}{\alpha} \arctan \frac{\alpha \sin(\omega t - \phi)}{1 - \alpha \cos(\omega t - \phi)} + B$ where $-1 \leq \alpha \leq 1$ is a tilting parameter. Adjusting the control parameters A, B, ω , and α makes it possible to generate different movements even though a robot has only a single chamber in the body for actuation. The different pressure channels can be set with different parameter values, allowing desynchronization and inter-robot variability as with the living worms.

B. Animals

We obtained California blackworms from Aquatic Foods & Blackworms Co. and from Ward’s Science. They are housed in a container filled with filtered water maintained at $\sim 4^\circ\text{C}$. Their diet consists of tropical fish flakes given to them once a week, while the water they inhabit is replaced every day. More information about rearing and maintenance is reported elsewhere [25], [26]. The experiments are performed after habituating the worms to room temperature water ($\sim 21^\circ\text{C}$). Studying these worms does not require approval from the institutional animal care committee.

IV. EXPERIMENTS

A. Single-Agent Locomotion

In this section we quantify the movement of single agents (robots and worms) under different conditions.

For the robots, we performed experiments with three different actuation patterns (gaits): (1) pure sine, (2) fast curl/slow uncurl (tilted sinusoid with $\alpha = 0.75$), (3) slow curl/fast uncurl (tilted sinusoid with $\alpha = -0.75$). For the Elastosil robots, we used $A = 10$ PSI and $B = 15$ PSI; for the Dragon Skin robots, because of their heterogeneity, we chose A on a channel-by-channel basis such that robots would empirically curl without breaking, from the range 15–20 PSI, and $B = 20$ PSI. We set $\phi_i = i\pi/4$ for the i th of eight channels for maximum desynchronization, and $\omega = \pi/5$ in all cases (period 10 seconds).

For both materials and each of the three gaits, we put five robots each through five actuation cycles. At the end of each half-cycle, when the robot was fully curled and fully uncurled, we recorded the position of the center of mass (CM) and the robot’s orientation. We conducted these experiments in air for the Elastosil robots and in water for the Dragon Skin ones.

Agent type	Condition	N	Displacement (mm)
Elastosil robot	Sine	25	26 ± 19
	FC/SU	25	37 ± 25
	SC/FU	25	53 ± 29
Dragon Skin robot	Sine	25	28 ± 19
	FC/SU	25	44 ± 36
	SC/FU	25	98 ± 50
Living worm	12°C	587	1.4 ± 1.9
	20°C	747	1.6 ± 2.0
	28°C	737	1.7 ± 1.2

TABLE I: CM displacement per full cycle (robots) or 1-second period (worms). Asterisks mark statistically significant differences between means (unpaired t-test): *: $p < 0.05$; **: $p < 0.01$; ***: $p < 0.0001$. FC/SU = fast curl/slow uncurl; SC/FU = slow curl/fast uncurl; N = number of data points.

The results (Fig. 3C, E) did not support a hypothesis that the orientation of the robot before actuation was predictive of the direction of its motion. Rather, the motion was consistent with a random walk. We explored this point further by using our empirical data to simulate longer walks using a resampling approach (Fig. 3B, D, F). The step size of the walk can be tuned by changing the control parameters (Fig. 3D, F; Table I).

For the living worms, single agents crawl using peristaltic waves of contraction of their circular and longitudinal muscles. The worms also have pairs of chaetae that help in locomotion and traction at the surface [27]. We analyzed worm motion by recording single worms moving freely in a Petri dish at three different temperatures (12°C , 20°C , and 28°C) and measuring their CM position and orientation at 1-second intervals. This study performed a reanalysis of data from experiments first reported in [5]. Each temperature tested three worms, each recorded until it first reached the edge of the dish. The results showed that unlike the robots, the single-worm motion is not well approximated as a straightforward random walk (Fig. 3B); a persistent random walk is a better model [28]. Here the temperature can be used to tune the effective speed or angular correlation.

For all three cases (both types of robots and living worms), the movement of the agent can be modulated by an observer (Table I): via the pressurization profile for the robots, and via the temperature for the worms.

B. Collective Locomotion

In this section we quantify the movement of groups of entangled agents (robots and worms) in different conditions.

Blackworm blobs have been observed to exhibit collective locomotion along a temperature gradient [4]. The mechanism of worm blob locomotion involves the worms inside the blob performing different functions depending on the location inside the blob. The worms at the top of the blob act as entangling agents to keep the blob cohesive. The worms in the movement direction of the blob (“pullers”) apply forward propulsion. Worms underneath the blob (“wigglers”) reduce friction with the substrate.

We performed experiments studying a worm blob’s ability to perform chemotaxis, a capability not previously reported.

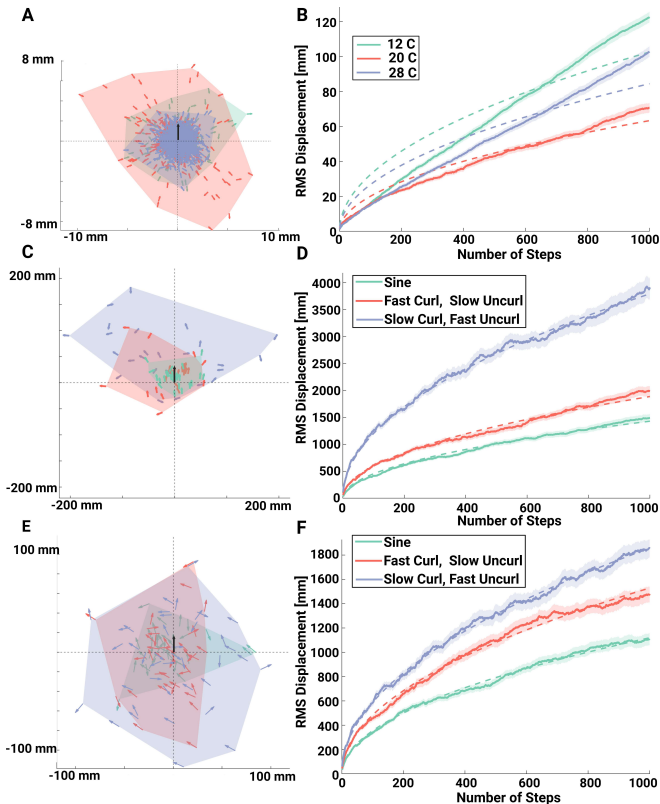


Fig. 3: Single-agent locomotion. (A–B) Living worms; (C–D) Dragon Skin robots; (E–F) Elastasil robots. (A, C, E) Position and angle changes resulting from one pressurization cycle (robots) or one 1-second period (worms). Each colored arrow shows the CM position and angle at the end of one such step, relative to the initial pose (black arrow). Each shaded region shows the convex hull around all steps observed for a given condition. (B, D, F) Root-mean-square (RMS) distance from the origin in resampling experiments, based on 100 trials, in each of which 1000 steps are randomly selected for each gait. Shaded error regions show the standard error of the mean. Dotted-line curves show RMS distance from origin for the theoretical random walks that best fit each of the experimental curves.

~ 200 worms were placed at one end of a 250mL Greiner Bio-One cell culture flask and allowed to form a blob. When food was introduced at the other end of the flask, the blob locomoted across to it following the chemical gradient (Fig. 4A). The chemotactic motion qualitatively resembled the previously observed thermotaxis.

We next explored the robots’ ability to achieve analogous collective locomotion. These experiments used Dragon Skin robots in water. We created robot blobs of n robots with m of them pressurized as entangling agents, and the other $n - m$ actuated with a sine gait using the parameters $A = 12$, $B = 12$, $\omega = \pi/5$. For $n = 3$, the blobs were arranged by hand. For $n = 16$, the blobs were allowed to self-assemble, by putting the unpressurized robots randomly on a surface and then pressurizing them, resulting in their entangling as they curl (Video 1). For $n = 8$, the blobs were allowed to

self-assemble and then were minimally adjusted by hand. To prevent plastic deformation of the worms, the pressure amplitude values were occasionally adjusted within a range of ± 3 psi, desynchronized with respect to phase. We explored locomotion for blobs with $\{n = 3, m = 1\}$, $\{n = 8, m = 5\}$, and $\{n = 16, m = 12\}$.

We empirically found that friction of the main blob mass against the substrate interfered with its motion when the entangling agents were statically pressurized, but actuating the entangling agents with a sine gait with $A = 2$ and $B = 22 \pm 3$ psi let the blob move more smoothly and quickly. This observation supports the earlier interpretation of the wiggler worms as aiding motion for living worm blobs by reducing friction [4].

Fig. 4 shows the robot blob’s progress over time qualitatively and quantitatively, for all blob sizes tested. The blob’s qualitative ability to achieve collective locomotion was present across this range of blob sizes, with no sensitive dependence on specific numbers of robots or pushers. Notably, for all n and m tested, the robot blob was driven by “pusher” agents on the trailing edge opposite the direction of motion, in contrast to the living blobs that were observed to be driven by “puller” agents [4].

C. Entanglement Strength

In this section we quantitatively characterize how the integrity of the blob is affected by the tightness of interaction of the agents, for both robots and living worms.

We first performed a quantitative experiment measuring pull-apart force as a function of inflation pressure, using a tensile testing machine (Instron 5544A). Because of the more uniform actuation response to pressurization shown by the Elastasil robots, we used those robots for these studies, and conducted them with the robots in air for experimental convenience. We created a blob by spreading out 16 robots on a surface and pressurizing them; the robots naturally entangle as they curl, without requiring careful initialization or manual adjustment. Eight worms were then attached to the top fixture of the testing machine while the other eight worms were attached to the bottom fixture (Fig. 5A). The load cell attached to the upper fixture measured the maximum pulling force during tensile tests until the blob is separated into two parts. The test was repeated 5 times each for different pneumatic input pressures, of 19, 21, 23, and 25 psi. The results (Fig. 5B) show how the maximum pulling force within a blob increases with higher pneumatic pressure.

These results are analogous to previous worm experiments showing qualitatively [25] and quantitatively [29] that a worm blob’s internal mechanical stress varies with the dissolved oxygen (DO) concentration in the surrounding water. In particular, experiments directly analogous to our tests above had a blob of ~ 250 worms entangle around a pair of serrated parts, with one part attached to a load cell and slowly raised while measuring the force with which the blob resists that motion [29]. The results showed that when the experiment was performed in air-saturated (normoxic) water with DO ~ 8 mg/L, vs. in oxygen-depleted water with DO

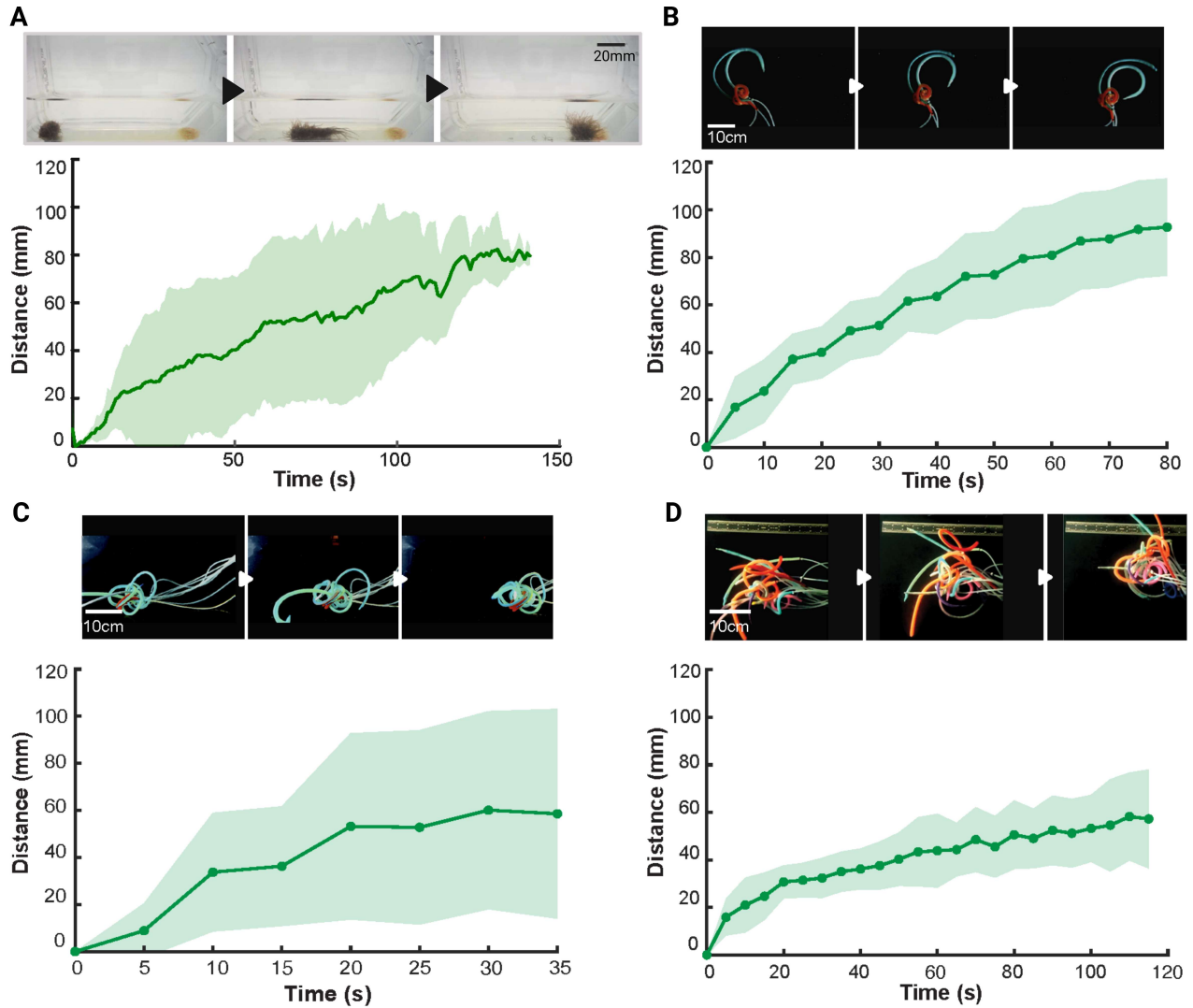


Fig. 4: Collective locomotion of worm and robot blobs. (A) ~ 200 living worms (side view). (B) Three robots, with two acting as pushers ($n = 3, m = 1$) (top view). (C) Eight robots, with three pushers ($n = 8, m = 5$) (side view). (D) 16 robots, with four pushers ($n = 16, m = 12$) (top view). The shaded regions in the plots show standard deviation of CM distance traveled ((A), three trials; (B–D), six trials). Actuation cycle period is 10 seconds for robots in all cases. See also Video 1.

~ 1 mg/L, the maximum force recorded was significantly different (Mann-Whitney U-test, $p=0.0022$) (Fig. 5C). That is, the entanglement force of the worm blob can be modulated by DO concentration, analogous to the entanglement force of the robot blob being modulated by inflation pressure.

We next investigated how the pull-apart force varies with the number of tangled robots being separated. In these tests, inflation pressure is kept fixed at 23 psi while the division of robots between the two half-blobs is varied, from the most asymmetric case with 1 on top and 15 below to the even division of 8-and-8 as in the first set of experiments. The results (Fig. 5D) show that the maximum force is greater when the blob is more evenly divided, consistent with an expectation that that condition corresponds to more points of entanglement between the two half-blobs, which must be broken to separate the halves. The force per top robot is approximately constant, consistent with the idea that robots

in such a setup can be modeled as parallel springs.

V. DISCUSSION

In this work, we have presented a physical system of high-aspect-ratio soft robots, capable of operation both in air and underwater, and exhibiting collective behaviors relying on physical entanglement. We demonstrated and characterized individual and collective locomotion, and tunable cohesive strength, for both robot and worm blobs. The analogous results in the two systems highlight the versatility of flexible entanglement-driven behavior across different scales and tasks.

In future work, we will explore other collective behaviors in which robot and worm blobs achieve tasks not possible for individuals. One immediate such behavior is collective transport, the act of moving objects too large for an individual to handle, a feat demonstrated by both natural and artificial swarms [30], [31]. In preliminary tests, we

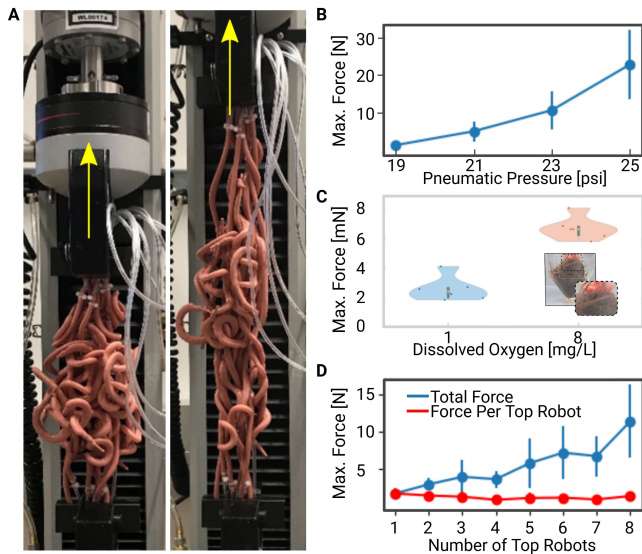


Fig. 5: Experiments measuring forces associated with pulling apart robot and worm blobs. (A) Experimental setup for robots with Instron machine. Robots are attached to upper and lower plates, and gradually pulled apart as a load cell measures the force required. (B) Maximum pulling force before separation, as inflation pressure is varied. (C) Similar test conducted with a living worm blob. Violin plot showing the maximum pulling force versus the water oxygenation level. The solid rectangles indicate the interquartile range, while the whiskers indicate the maximum and minimum values of the distribution. The individual data points are plotted as dots. Inset shows the worms entangled around the serrated part attached to the load cell. (Adapted from [29].) (D) Maximum pulling force before separation, as division of the 16 robots between the top and bottom plates is varied.

have demonstrated proof of concept for this task in both robot and worm blobs (Fig. 6). The approach we take is a composition of entangling and collective locomotion. If a blob self-assembles while an object is present, the agents can entangle with the object [23] at the same time as they entangle with each other. The blob can then execute collective locomotion as described above, and take the object with it as it moves. At a destination, the blob can release the object by disentangling: our robot blobs naturally disentangle when depressurized (Video 1), while worm blobs can be induced to disentangle via various methods such as applying an electric shock [32]. Future work will explore this and other possible behaviors in greater quantitative depth.

The robots and the living worms constitute two different systems that can be used as experimental probes of collective behaviors exhibited by entangled high-aspect-ratio agents. For a given behavior, noting which aspects match qualitatively in the two systems (e.g., “wiggler” agents aiding blob motion by reducing friction) and which differ (e.g., “puller” vs. “pusher” agents) may help identify what features are those critical for achieving that behavior. As another example, the detailed entangled geometry of a blob can

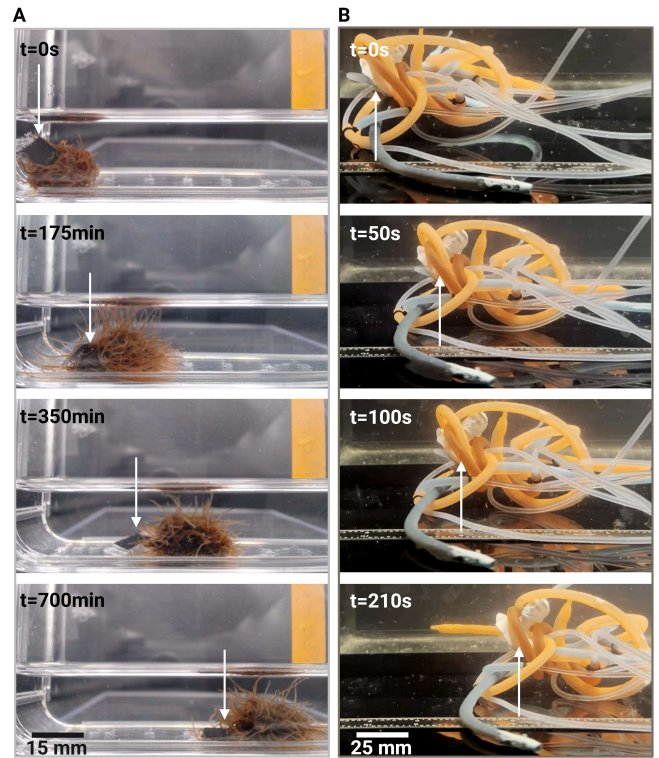


Fig. 6: Proof-of-concept demonstrations of collective transport, with worm and robot blobs. The blob entangles with an object, and carries it along as it undergoes collective locomotion. The cargo object is highlighted with an arrow in each case. (A) Worm blob (~ 200 worms) transporting a plastic mesh. (B) Robot blob ($n = 8, m = 6$) transporting a 3D-printed bust. See also Video 1.

be determined by tomography for both systems [23], [32], allowing evaluation of hypotheses about topological factors underlying tangling and untangling [22].

Future steps for the development of the physical robot system include incorporating embedded sensing into the robots, to allow them to evaluate their configuration and environment, and moving toward untethered versions with microfluidic logic [33]. These features will allow the system to move beyond the current limitations of external sensing and control and restricted movement, expand potential applications, and achieve fully autonomous collective behaviors by independent agents, as with the living blackworms.

ACKNOWLEDGMENT

We thank Kaitlyn Becker and Clark Teeple for assistance with experimental methods and equipment, and Ishant Tiwari and Nitesh Arora for sharing data sets from [5] and [29]. J.K. acknowledges funding support from National Research Foundation of Korea (NRF) funded by the Ministry of Education (2021R1A6A3A14044384). H.T. acknowledges the NSF Graduate Research Fellowship Program and the Georgia Tech’s President’s Fellowship. S.B. acknowledges funding support from NIH Grant R35GM142588; NSF Grants PHY-2310691; CMMI-2218382; and CAREER iOS-1941933.

REFERENCES

- [1] E. Bonabeau, M. Dorigo, and G. Théraulaz, *Swarm Intelligence: From Natural to Artificial Systems*. New York: Oxford University Press Inc., 1999.
- [2] S. Camazine, J.-L. Deneubourg, N. R. Franks, J. Sneyd, G. Theraulaz, and E. Bonabeau, *Self-Organization in Biological Systems*. Princeton University Press, 2001.
- [3] M. Brambilla, E. Ferrante, M. Birattari, and M. Dorigo, “Swarm robotics: A review from the swarm engineering perspective,” *Swarm Intelligence*, vol. 7, pp. 1–41, 2013.
- [4] Y. Ozkan-Aydin, D. I. Goldman, and M. S. Bhamla, “Collective dynamics in entangled worm and robot blobs,” *Proceedings of the National Academy of Sciences*, vol. 118, no. 6, p. e2010542118, 2021.
- [5] C. Nguyen, Y. Ozkan-Aydin, H. Tuazon, D. I. Goldman, M. S. Bhamla, and O. Peleg, “Emergent collective locomotion in an active polymer model of entangled worm blobs,” *Frontiers in Physics*, vol. 9, pp. 1–12, 2021.
- [6] A. Deblais, K. R. Prathyusha, R. Sinaasappel, H. Tuazon, I. Tiwari, V. P. Patil, and M. S. Bhamla, “Worm blobs as entangled living polymers: from topological active matter to flexible soft robot collectives,” *Soft Matter*, vol. 19, pp. 7057–7069, 2023.
- [7] H. Tuazon, C. Nguyen, E. Kaufman, I. Tiwari, J. Bermudez, D. Chudasama, O. Peleg, and M. S. Bhamla, “Collecting—Gathering Biophysics of the Blackworm *Lumbriculus variegatus*,” *Integrative and Comparative Biology*, vol. 63, no. 6, pp. 1474–1484, 06 2023. [Online]. Available: <https://doi.org/10.1093/icb/icad080>
- [8] M. Yim, W.-M. Shen, B. Salemi, D. Rus, M. Moll, H. Lipson, E. Klavins, and G. S. Chirikjian, “Modular self-reconfigurable robot systems: Challenges and opportunities for the future,” *IEEE Robotics and Automation Magazine*, vol. 14, no. 1, pp. 43–52, Mar. 2007.
- [9] M. W. Jorgensen, E. H. Ostergaard, and H. H. Lund, “Modular ATRON: Modules for a self-reconfigurable robot,” in *2004 IEEE/RSJ International Conference on Intelligent Robots and Systems (IROS)*(IEEE Cat. No. 04CH37566), vol. 2. IEEE, 2004, pp. 2068–2073.
- [10] B. Salemi, M. Moll, and W.-M. Shen, “SUPERBOT: A deployable, multi-functional, and modular self-reconfigurable robotic system,” in *2006 IEEE/RSJ International Conference on Intelligent Robots and Systems*, 2006, pp. 3636–3641.
- [11] H. Kurokawa, K. Tomita, A. Kamimura, S. Kokaji, T. Hasuo, and S. Murata, “Distributed self-reconfiguration of M-TRAN III modular robotic system,” *The International Journal of Robotics Research*, vol. 27, no. 3–4, pp. 373–386, 2008. [Online]. Available: <https://doi.org/10.1177/0278364907085560>
- [12] M. Shimizu, A. Ishiguro, and T. Kawakatsu, “Slimebot: A modular robot that exploits emergent phenomena,” in *Proceedings of the 2005 IEEE International Conference on Robotics and Automation*, 2005, pp. 2982–2987.
- [13] S. Li, R. Batra, D. Brown, H.-D. Chang, N. Ranganathan, C. Hoberman, D. Rus, and H. Lipson, “Particle robotics based on statistical mechanics of loosely coupled components,” *Nature*, vol. 567, pp. 361–365, 2019.
- [14] S. Ceron, M. A. Kimmel, A. Nilles, and K. Petersen, “Soft robotic oscillators with strain-based coordination,” *IEEE Robotics and Automation Letters*, vol. 6, no. 4, pp. 7557–7563, 2021.
- [15] J. Davey, N. Kwok, and M. Yim, “Emulating self-reconfigurable robots—design of the SMORES system,” in *Intelligent Robots and Systems (IROS), 2012 IEEE/RSJ International Conference on*, Vilamoura, Algarve, Portugal, October 7–12 2012, pp. 4464–4469.
- [16] C.-H. Yu, J. Werfel, and R. Nagpal, “Coordinating collective locomotion in an amorphous modular robot,” in *Proc. IEEE International Conference on Robotics and Automation (ICRA 2010)*, Anchorage, Alaska, 2010.
- [17] F. Mondada, G. C. Pettinaro, A. Guignard, I. W. Kwee, D. Floreano, J.-L. Deneubourg, S. Nolli, L. M. Gambardella, and M. Dorigo, “SWARM-BOT: A new distributed robotic concept,” *Autonomous Robots*, vol. 17, no. 2, pp. 193–221, 2004.
- [18] S. Yi, K. Sycara, and Z. Temel, “Reconfigurable robot control using flexible coupling mechanisms,” in *Robotics: Science and Systems*, 2023.
- [19] F. Pratisoli, A. Reina, Y. K. Lopes, C. Pincioli, G. Miyauchi, L. Sabattini, and R. Groß, “Coherent movement of error-prone individuals through mechanical coupling,” *Nature Communications*, vol. 14, no. 1, p. 4063, 2023. [Online]. Available: <https://doi.org/10.1038/s41467-023-39660-6>
- [20] M. Malley, B. Haghighat, L. Houel, and R. Nagpal, “Eciton robotica: Design and algorithms for an adaptive self-assembling soft robot collective,” in *2020 IEEE International Conference on Robotics and Automation (ICRA)*. IEEE, 2020, pp. 4565–4571.
- [21] A. Nilles, S. Ceron, N. Napp, and K. Petersen, “Strain-based consensus in soft, inflatable robots,” in *2022 IEEE 5th International Conference on Soft Robotics (RoboSoft)*. IEEE, 2022, pp. 789–794.
- [22] V. Patil, H. Tuazon, T. Chakraborty, J. Dunkel, and S. Bhamla, “Topological mechanics of living worm blobs,” APS March Meeting, 2022.
- [23] K. Becker, C. Teeple, N. Charles, Y. Jung, D. Baum, J. C. Weaver, L. Mahadevan, and R. Wood, “Active entanglement enables stochastic, topological grasping,” *Proceedings of the National Academy of Sciences*, vol. 119, p. e2209819119, 2022.
- [24] K. P. Becker, Y. Chen, and R. J. Wood, “Mechanically programmable dip molding of high aspect ratio soft actuator arrays,” *Advanced Functional Materials*, vol. 30, no. 12, p. 1908919, 2020.
- [25] H. Tuazon, E. Kaufman, D. I. Goldman, and M. S. Bhamla, “Oxygenation-Controlled Collective Dynamics in Aquatic Worm Blobs,” *Integrative and Comparative Biology*, vol. 62, pp. 890–896, 2022. [Online]. Available: <https://doi.org/10.1093/icb/icac089>
- [26] H. Tuazon, S. David, K. Ma, and S. Bhamla, “Leeches Predate on Fast-Escaping and Entangling Blackworms by Spiral Entombment,” *Integrative and Comparative Biology*, pp. 1408–1415, 2024. [Online]. Available: <https://doi.org/10.1093/icb/icac118>
- [27] C. Drewes and K. Cain, “As the worm turns: Locomotion in a freshwater oligochaete worm,” *The American Biology Teacher*, pp. 438–442, 1999.
- [28] H. i Wu, B.-L. Li, T. A. Springer, and W. H. Neill, “Modelling animal movement as a persistent random walk in two dimensions: expected magnitude of net displacement,” *Ecological Modelling*, vol. 132, no. 1, pp. 115–124, 2000. [Online]. Available: <https://www.sciencedirect.com/science/article/pii/S0304380000003094>
- [29] W. Savoie, H. Tuazon, I. Tiwari, M. S. Bhamla, and D. I. Goldman, “Amorphous entangled active matter,” *Soft Matter*, vol. 19, pp. 1952–1965, 2023.
- [30] S. Berman, Q. Lindsey, M. S. Sakar, V. Kumar, and S. C. Pratt, “Experimental study and modeling of group retrieval in ants as an approach to collective transport in swarm robotic systems,” *Proceedings of the IEEE*, vol. 99, no. 9, pp. 1470–1481, 2011.
- [31] M. Rubenstein, A. Cabrera, J. Werfel, G. Habibi, J. McLurkin, and R. Nagpal, “Collective transport of complex objects by simple robots: theory and experiments,” in *Proceedings of the 2013 International Conference on Autonomous Agents and Multi-Agent Systems*, 2013, pp. 47–54.
- [32] V. P. Patil, H. Tuazon, E. Kaufman, T. Chakraborty, D. Qin, J. Dunkel, and M. S. Bhamla, “Ultrafast reversible self-assembly of living tangled matter,” *Science*, vol. 380, pp. 392–398, 2023.
- [33] M. Wehner, R. L. Truby, D. J. Fitzgerald, B. Mosadegh, G. M. Whitesides, J. A. Lewis, and R. J. Wood, “An integrated design and fabrication strategy for entirely soft, autonomous robots,” *Nature*, vol. 536, no. 7617, pp. 451–455, 2016. [Online]. Available: <https://doi.org/10.1038/nature19100>